

(FINAL)  
ANNUAL TECHNICAL REPORT

Kinetics of Diffusional Droplet Growth in a Liquid/Liquid Two-Phase  
System

M.E. Glicksman and V.E. Fradkov  
Materials Science & Engineering Department  
Rensselaer Polytechnic Institute  
Troy, New York 12180-3590

NASA Agreement No. NCC8-54

June 30, 1996

## Background

Experimental techniques for measuring the kinetic behavior of liquid-liquid droplet dispersions held isothermally in thin cuvettes were developed at the Space Science Laboratory, Low Gravity Research Division, NASA Marshall Space Flight Center. The observational method, based on optical holography, was developed originally by Dr. D.O. Frazier and his scientific staff, including W.K. Witherow, B.R. Facemire, J.P. Downey, and J.R. Rogers. This holographic data set at MSFC is the largest set of quantitative coarsening data available. The Principal Investigator (M.E. Glicksman) and the Co-Principal Investigator (V.F. Fradkov), both at Rensselaer Polytechnic Institute, were asked originally by NASA to assist scientists at MSFC in interpreting the observed coarsening kinetics as the liquid-liquid system (isopycnic phases consisting of succinonitrile-rich drops in a water-rich matrix) was annealed over long periods of time.

Cooperative research activities originally initiated under NASA contract NAG8-864 included developing novel numerical techniques for predicting the lifetimes of individual droplets located within a specified area of a hologram. These predictions were based on solving the multiparticle diffusion problem in two spatial dimensions, subject to certain boundary conditions applied to the droplets as 3-dimensional objects. This so-called *mixed-dimensional* interpretation of the coarsening kinetics, as observed by Frazier *et al.*, proved extremely beneficial in correlating the holographic observations with a theoretical framework. This collaborative research work between MSFC and Rensselaer appeared subsequently as the following two archival papers:

- 1) J.R. Rogers, J.P. Downey, W.K. Witherow, B.R. Facemire, D.O. Frazier, V.E. Fradkov, S.S. Mani, and M.E., Glicksman, "Coarsening of Three-Dimensional Droplets by Two-Dimensional Diffusion: Part I Experiment," *Journal of Electronic Materials*, Vol. 23, No. 10, pp 999-1006, (1994).
- 2) V.E. Fradkov, S.S. Mani, M.E., Glicksman, J.R. Rogers, J.P. Downey, W.K. Witherow, B.R. Facemire, and D.O. Frazier, "Coarsening of Three-Dimensional Droplets by Two-Dimensional Diffusion: Part II Theory," *Journal of Electronic Materials*, Vol. 23, No. 10, pp 1007-1013, (1994).

## **Annual Progress**

The Principal Investigator and Co-Principal Investigator have developed a novel numerical method for performing multiparticle diffusion calculations that permit statistical analysis of the NASA/MSFC droplet holograms. The new method uses instantaneous "snap-shots" calculations of many diffusionally interacting particles (up to several thousand). Heretofore, time-marching techniques were needed to determine the coarsening rates in multiparticle clusters. Such time-dependent calculations were so computationally laborious that the kinetic behavior of only a few hundred particles could be determined even with the largest computers available. Now clusters containing thousands of particles can be assessed numerically with only modest computing power.

The theoretical basis for the new method, based on linear perturbation analysis, along with some initial results obtained for three-dimensional clusters has been published recently. This paper, attached to this report in pre-print form, appears as Appendix 1, is entitled:

"Coarsening kinetics in finite clusters," *Physical Review E*, Vol. 53, No. 4, pp. 3925-3932, (1996).

The new method, detailed in Appendix 1, specifically permits assessment of the diffusion screening distance (Debye length) in two-phase mixtures, such as being studied by Frazier *et al.* at MSFC. The availability of the MSFC hologram data base for droplet coarsening can be analysed further by applying the methods disclosed herein.

The Co-Principal Investigator, Dr. Fradkov, is currently spending a 12-week period of the Summer, 1996, at MSFC, working with the NASA scientists in Dr. Frazier's Branch. Further details of the application of these methods by MSFC scientists are being worked out during the visit to Huntsville, Alabama, by Dr. Fradkov. The Principal Investigator also plans at least one trip to MSFC during the Summer of 1996 to interact directly with the MSFC scientists.

## **Future Plans**

If the current cooperative agreement is funded for 1997 and extended for one year beyond the requested extension date of September 30, 1996, the following plan of research activities will be followed:

- Multiparticle calculations will be provided for studying higher volume fractions than investigated for MSFC during 1996. Our initial study, as detailed in Appendix 1, was limited to a *maximum* volume fraction (in three dimensions) of 0.01. The Principal Investigator feels that this restriction can be relaxed by using novel techniques that extend these numerical computations to "dipolar" order, as compared to the "monopolar" computations accomplished to date at low volume fractions. This approach is especially valid for analyzing the MSFC droplet coarsening hologram data base, which require solving the diffusion equation in only two space dimensions. The equation set for solving the diffusion field for large two dimensional clusters is not as difficult to invert as is the one for a three dimensional cluster. Implementing this plan will require cooperative decisions with the cognizant NASA scientists at MSFC.

- The Principle Investigator would attempt to implement some fast inversion methods for solving the "snap shot" diffusion equation to dipolar order. If successfully accomplished this development would lead to coarsening kinetic coefficients useful for analyzing data obtained at higher area fractions in two dimensions. This element of our future work would be carried out cooperatively with applied interested mathematicians here at Rensselaer Polytechnic Institute, at the Courant Institute, New York, NY, and at the National Institute of Standards and Technology, Gaithersburgh, Maryland.

## APPENDIX 1

# Coarsening Kinetics in Finite Clusters

V.E. Fradkov, M.E. Glicksman, S.P. Marsh \*

Rensselaer Polytechnic Institute  
Materials Engineering Department  
Troy, NY 12180-3590

\*Naval Research Laboratory  
Physical Metallurgy Branch  
Washington, DC 20375

## Abstract

We address the problem of diffusional interactions in a finite sized cluster of spherical particles for volume fractions,  $V_V$ , in the range 0–0.01. We determined the quasi-static monopole diffusion solution for  $n$  particles distributed at random in a continuous matrix. A global mass conservation condition is employed, obviating the need for any external boundary condition. The numerical results provide the instantaneous (snapshot) growth or shrinkage rate of each particle, precluding the need for extensive time-dependent computations. The close connection between these snapshot results and the coarse-grained kinetic constants are discussed. A square-root dependence of the deviations of the rate constants from their zero volume fraction value is found for the higher  $V_V$  investigated. This behavior is consistent with predictions from diffusion Debye-Hückel screening theory. By contrast, a cube-root dependence, reported in earlier numerical studies, is found for the lower  $V_V$  investigated. The roll-over region of the volume fraction where the two asymptotics merge depends on the number of particles,  $n$ , alone. A theoretical estimate for the roll-over point predicts that the corresponding  $V_V$  varies as  $n^{-2}$ , in good agreement with the numerical results.

## I. Introduction

Diffusional coarsening represents an important and commonly observed kinetic process in microstructural evolution. Coarsening can occur among several microstructural constituents ranging from the primary phases to widely dispersed precipitates. The wide range of volume fractions,  $V_v$ , encountered in phase coarsening, makes it essential to have a fundamental theory of coarsening which treats the volume fraction as an input parameter of the microstructure. The classic coarsening theory developed by Todes [1] and Lifshitz and Slyozov [2] (TLS theory) is limited to infinitesimally small volume fractions. To date, scores of papers have been published attempting to extend TLS theory to finite volume fractions intrinsic to real microstructures. Several excellent reviews have been published surveying these models along with relevant experiments [3-5]. Nonetheless, even finding the initial corrections to TLS theory in the limit of small volume fractions remains an open question. Specifically, the analytical theory for *infinite* systems suggested by Marqusee and Ross [6] and Marqusee [7], based on the diffusion analog of the Debye-Hückel screening effect, leads to deviations from TLS in the coarsening rate, which are proportional to  $V_v^{1/2}$ . By contrast, several numerical analyses [8,9] dealing with *finite* systems clearly show that this deviation is, instead, proportional to  $V_v^{1/3}$ . The purpose of the present paper is to analyze how the coarsening rates change in a finite cluster of a specified particle density. We will show numerically that both  $V_v^{1/2}$  and  $V_v^{1/3}$  behaviors may occur, depending on the number of particles comprising the cluster and its volume fraction. The crossover between these behaviors will be derived analytically using the Debye-Hückel screening concept.

## II. Theoretical Background: Mean-Field Approaches

The simplest model of coarsening in infinitesimally sparse systems [1] assumes that all precipitate particles remain spherical and remote from each other, and that their positions remain stationary. The description of isothermal coarsening is given in [1] in terms of the radius distribution function,  $F(R,t)$ , where  $R$  and  $t$  are the particle radius and the time. The norm of  $F(R,t)$  is based on the total number of particles per unit volume,  $N_v$ , that is

$$\int_0^\infty F(R,t) dR = N_v. \quad (1)$$

With this normalization, the volume fraction,  $V_v$ , of the dispersed phase is given by

$$V_v \equiv \int_0^\infty F(R,t) \frac{4\pi}{3} R^3 dR = \frac{4\pi}{3} N_v \langle R^3 \rangle. \quad (2)$$

Supersaturation of the matrix solution is assumed to be small, so that nucleation of new particles is precluded. The continuity equation for particles in size space is

$$\frac{\partial F}{\partial t} + \frac{\partial}{\partial R} [v(R) \cdot F] = 0, \quad (3)$$

where  $v(R)$  is the time-rate of change of the radius,  $R$ , of a particle. To obtain  $v(R)$ , further simplifying assumptions were made: (a) the kinetics of coarsening is limited by volume diffusion; and (b) the diffusion is quasi-static. Therefore, the diffusion equation describing the concentration field,  $c(\mathbf{r})$ , in the matrix phase reduces to the Laplace equation

$$\nabla^2 \varphi = 0, \quad (4)$$

where  $\varphi = (c - c_0)/c_0$  and  $c_0$  is the equilibrium solubility. The boundary conditions at the surface of the  $i$ -th particle are specified through the Gibbs-Thomson local equilibrium relation

$$\varphi_i = \frac{\lambda}{R_i}, \quad (5)$$

where  $\lambda$  is the capillary length given by

$$\lambda = \frac{2\gamma\Omega}{k_B T}. \quad (6)$$

Here,  $\gamma$  is the particle-matrix specific interfacial energy,  $\Omega$  is the atomic volume of the dispersed phase,  $k_B$  is the Boltzmann constant, and  $T$  is temperature. Additionally, anisotropy of the interfacial energy and strain effects were ignored.

The solution to eq. (4), subject to the boundary conditions (5) at the interface of each particle, may be written in the form of the Coulomb potential<sup>1</sup>,

$$\varphi(\mathbf{r}) = \sum_i \frac{\lambda B_i}{|\mathbf{r} - \mathbf{r}_i|} + \varphi_\infty, \quad (7)$$

where  $\varphi_\infty$  is the background matrix diffusion potential, assumed uniform throughout the matrix phase;  $\mathbf{r}$  is a field point always in the matrix;  $\mathbf{r}_i$  locates the center of the  $i$ -th particle. The diffusion analog of electrostatic charge is the volume flux per steradian,  $B_i$ , given by

$$B_i = \left( 1 - \frac{R_i}{R^*} \right), \quad (8)$$

where the critical radius,  $R^*$ , is given by

$$R^* = \frac{\lambda}{\varphi_\infty}. \quad (9)$$

The time-rate of change of the radius,  $v(R)$ , used in eq. (3), is directly connected to  $B_i$  as

$$v(R_i) = -\frac{2\lambda D c_0 \Omega}{R_i^2} B_i. \quad (10)$$

Equation (8) provides the values of  $B_i$ , but the value of  $\varphi_\infty$  remains unknown. Todes suggested using the global conservation of volume of the dispersed phase, neglecting changes in the supersaturation within the matrix phase [1]:

---

<sup>1</sup> The solution given by eq. (7) is a monopole approximation, where the particles are treated as point sources and sinks. This is justified by the large distances between the particles compared to their radii.



$$\frac{d}{dt} \int_0^{\infty} F(R,t) \cdot \frac{4\pi}{3} R^3 dR \equiv \int_0^{\infty} \frac{\partial}{\partial t} F(R,t) \cdot \frac{4\pi}{3} R^3 dR = 0. \quad (11)$$

Using the continuity equation to substitute for  $\partial F/\partial t$ , one obtains

$$\varphi_{\infty} = \frac{\int_0^{\infty} F(R,t) dR}{\int_0^{\infty} F(R,t) R dR} \equiv \frac{1}{\langle R \rangle}, \text{ or } R^* = \langle R \rangle. \quad (12)$$

Todes also introduced a dimensionless variable  $\rho = R/R^*$ . The dimensionality of the diffusion-limited coarsening process implies that

$$R^* = \alpha (2\lambda D c_0 \Omega t)^{1/3}, \quad (13)$$

where  $\alpha$  is a dimensionless kinetic coefficient to be defined later. Todes then found a one-parameter family of self-similar solutions for the distribution function,  $F(R,t)$ , given by the product-function form

$$F(R,t) = \frac{N_v(t)}{R^*(t)} f(\rho, \alpha). \quad (14)$$

With eq.(14), the continuity equation, (3), reduces to the following O.D.E.

$$\frac{df}{f} = \frac{-4\rho^3 + (6/\alpha^3)(1-\rho) d\rho}{(3/\alpha^3)(1-\rho) + \rho^3} \frac{d\rho}{\rho}. \quad (15)$$

The number of real roots of the denominator,  $\mathcal{D} = (3/\alpha^3)(1-\rho) + \rho^3$ , on the r.h.s. of eq.(15) depends on the value of  $\alpha$ , which in turn influences the qualitative behavior of the solution to eq.(15). Figures 1a-c show the three possible behaviors of the denominator. For  $\alpha > (2/3)^{2/3}$ , figure 1-a, there is no real root of the denominator, and the solution to eq.(15) is analytic up to infinity. This solution, however, causes a logarithmic divergency of the integral for the total volume of the particles. Truncating the logarithmic tail, however, destroys self-similarity of the distribution function,  $f(\rho)$ , because the relative density of particles at large  $\rho$  values is gradually exhausted. For  $\alpha < (2/3)^{2/3}$ , figure 1-c, the solution must be restricted between zero and the first positive root of the denominator and set equal to zero beyond, in order to prevent singular behavior of the distribution function at the roots of the denominator. These solutions are, however, unstable with respect to appearance in the system of a particle outside of the permitted range as a result of coalescence. Lifshitz and Slyozov [2], therefore, stated that the only stable solution to the continuity equation, (3), corresponds to such a value of  $\alpha$  that makes the two positive roots of the denominator coincide, figure 1-b. That implies

$$\alpha_{TLS} = (2/3)^{2/3}. \quad (16)$$

It is important to note that although the TLS solution to coarsening kinetics does not depend formally on the value of the volume fraction,  $V_v$ , it is *not, in fact, extensible to any*

*non-zero volume fraction.* The restriction of the TLS solution to zero volume fraction is a consequence of the contradiction between the infinite extent of the Laplace diffusion field and the total neglect of direct interactions among the particles. This contradiction manifests itself even stronger in two dimensions, where an analogous TLS theory cannot even be developed without imposing some arbitrary cutoff radius to the diffusion field, due to its logarithmic far-field behavior for each individual particle [8, 9].

There are two general approaches used to incorporate the influence of volume fraction on coarsening kinetics. The earliest approaches were based on arbitrary restriction of the extent of the interparticle diffusional interactions to the average interparticle separation (see [17] for a review). In sparse systems the nearest neighbors, of course, cannot shield the Laplacian field. Theories based on models using interparticle distance for the cutoff are generally in poor agreement with experiment and numerical simulations [3, 4, 17]. For higher volume fractions,  $0.1 < V_v < 0.6$ , however, direct screening by nearest neighbors becomes more reasonable, but generally the models that use a single cutoff radius do not provide meaningful results for the specified range of volume fractions (see ref. [10] for a review).

Marqusee and Ross [6] and Marqusee [7], by contrast, restricted the extent of the Laplacian diffusion field by taking into account screening effects in active two-phase media containing a distribution of diffusional sources and sinks. Instead of the Laplace equation, Marqusee and Ross obtained the Poisson equation for the spatially coarse-grained background diffusion potential,  $\phi$ , namely

$$\nabla^2 \phi = -4\pi\sigma, \quad (17)$$

in which the source/sink density,  $\sigma$ , in the matrix space surrounding a particle is given by

$$\sigma(\mathbf{r}) = \int_0^\infty \lambda B \cdot F(R, t) dR = \int_0^\infty (\lambda - R\phi(\mathbf{r})) F(R, t) dR. \quad (18)$$

Note that here the background potential in Eq.(8),  $\phi_\infty$ , is replaced by the coarse-grained potential,  $\phi$ , consistent with Debye's approach. Carrying out the indicated integration on the right-hand side of eq. (18) gives

$$\sigma(\mathbf{r}) = N_v \lambda - N_v \langle R \rangle \phi(\mathbf{r}). \quad (19)$$

where  $N_v$  and  $\langle R \rangle$  are defined by eqs. (1) and (12), respectively. Substituting eq. (19) into eq. (17) yields the diffusion analog of the Debye-Hückel equation, namely

$$\nabla^2 \phi - \kappa^2 (\phi - \phi_\infty) = 0, \quad (20)$$

where

$$\kappa^2 = 4\pi N_v \langle R \rangle, \quad (21)$$

and

$$\phi_\infty = \lambda / \langle R \rangle. \quad (22)$$

Equation (20) is well known from the theories of ionic plasmas and electrolytes, where it is used to describe the electrostatic field developed in an active medium containing a distribution of quantized charges. In these theories, the second term on the l.h.s. of eq. (20) describes the space charge density caused by spatial redistribution of the charges, in order to minimize the electrostatic energy. In the case of diffusional coarsening, however, the positions of the “charges” (diffusional source/sink strengths) are fixed, but their values, the  $B_i$ ’s, depend on the *local* background potential,  $\phi(\mathbf{r})$ , consistent with eq. (8).

The solution to eq. (20) subject to the boundary conditions, eq. (5), is in the form of a Yukawa potential

$$\phi(\mathbf{r}) = \sum_i \frac{\lambda B_i}{|\mathbf{r} - \mathbf{r}_i|} \exp(-\kappa \cdot |\mathbf{r} - \mathbf{r}_i|) + \phi_\infty, \quad (23)$$

where now the  $B_i$ ’s are defined as

$$B_i = \left(1 - \frac{R_i \phi_\infty}{\lambda}\right) (1 + \kappa R_i) = B_i^{TLS} (1 + \kappa R_i). \quad (24)$$

$B_i^{TLS}$  denotes the dimensionless volume fluxes (per steradian) for particles in an infinitesimally dilute system, as given in the TLS theory by eq. (8). The coefficient  $\kappa$  is the reciprocal of the diffusional analog of the Debye screening length. It represents the natural cut-off distance for direct particle interactions via the diffusion field, beyond which the particles are isolated from each other by the intervening two-phase medium. As seen from eq. (24),  $\kappa R_i$  expressly captures the deviations in the rate of particle size evolution from the TLS limit. It is possible to use the same global stability analysis introduced by Lifshitz and Slyozov [2] to obtain the characteristic kinetic constant,  $\alpha$ , which determines the overall rate of coarsening as defined in eq. (13) (see [6] for details):

$$\alpha(V_v) = \alpha_{TLS} (1 + 0.740 V_v^{1/2} + \text{H.O.T.}), \quad (25)$$

where  $\alpha_{TLS} = (2/3)^{2/3}$  is the TLS-limit for infinitesimally diluted systems ( $V_v = 0$ ). Equation (25) shows that the average particle size grows more rapidly than in the TLS limit. Moreover, this correction, reflecting diffusional Debye screening, implies other first-order corrections, including the broadening of the size distribution function and the difference between the average and the critical radii; all these corrections are proportional to the square root of the volume fraction.

### III. Kinetic Properties of Finite Coarsening Systems

There are four physically distinct metric scales in any *finite* coarsening cluster, i.e., a finite number of particles confined to a finite volume: 1) the size of the particles, as characterized by  $\Lambda_R \approx \langle R \rangle$ ; 2) the interparticle spacing, as characterized by  $\Lambda_N \approx N_v^{-1/3}$ , where  $N_v$  is the total number of particles per unit volume, eq. (1); 3) the Debye screening

radius,  $\Lambda_D \equiv \kappa^{-1}$ ; and 4) the extent of the total coarsening system,  $\Lambda_{\text{tot}}$ , as defined for a “spherical cluster” by  $\Lambda_{\text{tot}} = (4\pi/3)^{-1/3} (n/N_V)^{1/3}$ , where  $n$  is the total number of particles remaining at a given time. Note, it is always assumed that the cluster is locally homogeneous and spatially isotropic, and that the overall size of the cluster,  $\Lambda_{\text{tot}}$ , is time independent. These assumptions permit one to establish an analog of the volume fraction for a finite cluster of particles,

$$V_V = \frac{\sum_{i=1}^n \frac{4\pi}{3} R_i^3}{\frac{4\pi}{3} \Lambda_{\text{tot}}^3}, \quad (26)$$

where the denominator in eq. (26) provides an estimate of the spherical cluster volume .

By contrast with infinite systems, finite systems lack *uniform* asymptotics, because any finite system ultimately achieves its end state as a single particle in finite time. Finite systems, instead, may only exhibit *intermediate* asymptotics. By this we mean that the coarse-grained average over time of these cluster parameters becomes identical to those in self-similar infinite systems, even though the instantaneous values of the time-dependent parameters of finite clusters may fluctuate. All continuum coarsening theories, however, exclusively yield quantities that are equivalent to the coarse-grained averages over time for finite clusters. Specifically, therefore, the coarse-grained *intensive* length scale parameters, viz.  $\Lambda_M$ ,  $\Lambda_R$ , and  $\Lambda_D$ , are expected to scale with time as predicted by continuum coarsening theories.

Weins and Cahn [11] were the first to estimate the diffusional interactions among a few particles comprising a small coarsening cluster. Later Voorhees and Glicksman [12, 13] extended Weins and Cahn’s analysis to hundreds of particles by using periodic boundary conditions, and adapted Ewald sums to improve the convergence of the numerical calculations. In finite systems, coarsening always occurs via two distinct but related processes: the *continuous* evolution of the particle radii, and the *discontinuous* (instantaneous) disappearances of the smallest particles. The coarse-grained time averages depend on both processes. Specifically, during the continuous process, the average size of the particles decreases (along with the total interfacial area), whereas the instantaneous disappearances cause the average size to increase. The actual evolution of the average radius consists of smoothly falling segments connected by vertical jumps whenever a particle disappears, as observed in computer simulations [13, 15]. The coarse-grained average changed with time as  $t^{1/3}$ , according to the TLS prediction.

A recent simulation and experimental study of coarsening in a finite clusters of three-dimensional particles interacting through two-dimensional diffusion field [14,15] shows similar discontinuous behavior of the average radius, whereas the coarse-graining behavior of the average particle radius exhibited a power law of  $t^{1/4}$ , characteristic of the continuum coarsening prediction for the mixed-dimensional case (see figure 2). Thus,

experiments confirm and simulations show that the coarse-grained intermediate asymptotic behavior of real, i.e. finite, coarsening systems is consistent with theoretically predicted asymptotic power laws from continuum theories.

Normally, the numerical data required for coarse-grained averaging are obtained by time-dependent computer simulations. Following such procedures for large clusters (tens of thousands of particles) is computationally intensive. There would be a great advantage in large finite systems to limiting the numerical simulation to a “snapshot” analysis of the rate of change of  $\langle R \rangle$  along the continuous segments. It is unclear, however, how the instantaneous slopes,  $v(R_i)$ , defined by eq. (10), are related to the coarse-grained average time dependence of  $\langle R \rangle$ . One can show, using first-order perturbation theory, that the relative change in the kinetic constant,  $\alpha$ , from the Lifshitz-Slyozov stability analysis is proportional to the relative change in the growth rate,  $v(R_{max})$ , for the largest particle within the TLS-distribution, induced by any small perturbation. Specifically, if a small disturbance to the particle growth rates,  $\epsilon(R)$ , is introduced as

$$v(R) = v_{TLS}(R) \cdot [1 + \epsilon(R)], \quad (27)$$

where  $v_{TLS}$  is the non-perturbed value given by the TLS theory, eq.(10). The denominator,  $\mathcal{D}$ , in eq. (15), becomes

$$\mathcal{D} = \rho^3 - \beta(\rho-1)(1+\epsilon). \quad (28)$$

where  $\beta = 3/\alpha^3$ . Following the procedure set out in the earlier section, *Theoretical Background*, we find the eigenvalue for  $\beta$  and the maximum value of  $\rho$  by solving the equation set  $\mathcal{D}=0$  and  $\mathcal{D}'=0$ . Seeking first-order corrections to the eigenvalue, we write

$$\beta = \beta_{TLS} + \delta\beta \quad (29)$$

and

$$\rho = \rho_{TLS} + \delta\rho. \quad (30)$$

where  $\rho_{TLS} = 3/2$ , and  $\beta_{TLS} = 27/4$ .

Keeping only first-order terms, we find

$$\mathcal{D} = -\delta\beta/2 - (27/8)\epsilon = 0 \quad (31)$$

where  $\epsilon$  is evaluated at  $\rho_{TLS} = 3/2$ . This results in  $\delta\beta = - (27/4)\epsilon$ , and

$$\alpha = \alpha_{TLS} \cdot \left[ 1 + (3/16)^{1/3} \epsilon(R_{max}^{TLS}) \right]. \quad (32)$$

Here,  $R_{max}^{TLS} = (3/2)\langle R \rangle$  and  $\alpha_{TLS} = (2/3)^{2/3}$  are the non-perturbed values given by the TLS theory. For example, if the perturbation,  $\epsilon(R)$ , is caused by diffusional Debye screening, eq. (24), then eq. (32) transforms to eq. (25) from the analysis by Marqusee and Ross [7].

The second equation,  $\mathcal{D}'=0$ , may be written as  $\partial\mathcal{D}/\partial\delta\rho=0$ , or, keeping first-order terms,

$$\mathcal{D}' = 6\rho_{TLS}\delta\rho - \delta\beta - \beta_{TLS}\epsilon - \beta_{TLS}(\rho_{TLS}-1)\epsilon' = 0. \quad (33)$$

This gives the correction in  $\rho_{max}$ , which however depends not on  $\epsilon$  but on  $\epsilon' = \partial\epsilon/\partial\delta\rho$ ,

$$\delta\rho = (3/8) \epsilon'. \quad (34)$$

The snapshot numerical analysis, to be discussed below, is capable of providing the  $\epsilon(R)$  values for each particle in the cluster. In a finite cluster, however, one does not have a statistically valid representation of enough particles at  $R_{max}$  to guarantee an accurate estimate of  $\epsilon(R_{max})$ . *Consequently, we will average the perturbations over the entire system of particles, using the assumption that the global average,  $\langle\epsilon(R)\rangle$ , reflects the behavior of  $\epsilon(R_{max})$ .* This assumption is a rather likely outcome of the self-similar behavior we are discussing.

#### IV. "Snapshot" Numerical Analysis

The mathematical formulation for the present numerical study is based on the monopole approximation to the quasi-static diffusion solution shown in eq. (7). The particle growth rates were calculated for each individual particle in the cluster according to eq. (7), using the exact monopole expressions for the dimensionless diffusional source/sink strengths,  $B_i$ 's, namely

$$B_i = \left[ 1 - \frac{R_i}{\lambda} \left( \varphi_\infty + \sum_{j=1, j \neq i}^n \frac{B_j}{|r_j - r_i|} \right) \right]. \quad (35)$$

Here  $n$  is the total number of particles in the cluster,  $\lambda$  is a capillary length defined in eq. (6), and the expression in the parenthesis represents the local analog of the background diffusion potential used in the TLS theory, eq. (8). Equation (35) represents a set of  $n$  linear equations with  $n+1$  unknowns, viz., the  $B_i$ 's and  $\varphi_\infty$ . One additional equation is needed to close the system. In previous simulations such an equation was provided by an external boundary condition, e.g., the periodicity condition used in [9, 13]. In the present work we employ, instead, a conservation equation for the total volume of the particles, as suggested in [11, 15]:

$$\sum_{i=1}^n B_i = 0. \quad (36)$$

A version of the Gauss-Seidel iterative algorithm was employed for solving the set of equations given by eqs. (35) and (36), which equations may be written in matricial form as

$$\begin{bmatrix} \frac{\lambda}{R_1} & \frac{\lambda}{|r_1 - r_2|} & \frac{\lambda}{|r_1 - r_3|} & \dots & \dots & \dots & 1 \\ \frac{\lambda}{|r_1 - r_2|} & \frac{\lambda}{R_2} & \frac{\lambda}{|r_2 - r_3|} & \dots & \dots & \dots & 1 \\ \frac{\lambda}{|r_1 - r_3|} & \frac{\lambda}{|r_2 - r_3|} & \frac{\lambda}{R_3} & \dots & \dots & \dots & 1 \\ \dots & \dots & \dots & \dots & \dots & \dots & 1 \\ \dots & \dots & \dots & \dots & \dots & \dots & 1 \\ \dots & \dots & \dots & \dots & \dots & \dots & 1 \\ 1 & 1 & 1 & 1 & 1 & 1 & 0 \end{bmatrix} \cdot \begin{bmatrix} B_1 \\ B_2 \\ B_3 \\ \dots \\ \dots \\ \dots \\ \phi_\infty \end{bmatrix} = \begin{bmatrix} \frac{\lambda}{R_1} \\ \frac{\lambda}{R_2} \\ \frac{\lambda}{R_3} \\ \dots \\ \dots \\ \dots \\ 0 \end{bmatrix}. \quad (37)$$

A linear projection to  $n \times n$  subspace was employed to eliminate the last row and column and make the matrix, eq. (37), suitable for applying the classic Gauss-Seidel linear solver.

The cluster parameters in the “snapshot” simulation are: the set of  $n$  particle center coordinates,  $\{r_i\}$ , and the set of  $n$  particle radii,  $\{R_i\}$ , both of which are measured in units of  $\lambda$ . The  $n$  particle center coordinates in this simulation are chosen randomly inside a sphere of radius  $\Lambda_{\text{tot}}$ . Each particle was assigned a radius randomly distributed around the average value  $\langle R \rangle = \Lambda_R$  according to various distributions. Specifically, we used the TLS particle size distribution and a rectangular distributions of various widths. An influence of the particle size distribution on the kinetic results was not observed. The particles are not allowed to overlap. This restriction results in some correlation between particle sizes and positions, which tends to vanish with decreasing volume fraction. The volume fraction itself was varied by changing the ratio  $\Lambda_R^3 / \Lambda_{\text{tot}}^3$ , according to eq. (26), while maintaining fixed relative positions and radii of the particles. Specifically, we proportionally changed all the interparticle distances and, consequently, changed the size of the cluster and the volume fraction, whereas the particle radii remained constant.

## V. Results and Discussion

Figure 3 shows the dependence on the volume fraction of the observed relative deviations,

$$\Delta(V_r) = \frac{\langle v(R, V_r) \rangle - \langle v(R, 0) \rangle}{\langle v(R, 0) \rangle}, \quad (38)$$

in the values of the rate of change of the average radius,  $\langle v(R, V_r) \rangle$ , compared to that for zero volume fraction,  $\langle v(R, 0) \rangle$ . The values at non-zero volume fractions were obtained from the snapshot calculations, using eq.(37), whereas the zero volume fraction term is obtained from the TLS expression, eq. (8). The results are shown for clusters containing 10, 100, and 1000 particles. The deviations are plotted on log-log coordinates vs. the

volume fraction,  $V_v$ , given by eq. (26), which was varied for each calculation by changing the ratio  $\Lambda_R^3/\Lambda_{\text{tot}}^3$ , as described above. There appear to be two distinguished limits for the slopes, representing the exponents of the leading-order corrections introduced by the volume fraction. For the higher ranges of volume fraction the exponent is 1/2, in agreement with Debye screening theory, eq.(24). Combining eqs. (2), (8), (10), (21), and (24) with the definition of  $\Delta$ , eq.(38), we obtain the expression for  $\Delta$  in terms of the volume fraction,

$$\Delta = \left( \frac{1 - \mu_{-1}}{\mu_{-1} - \mu_{-2}} \right) \left( \frac{3}{\mu_3} \right)^{1/2} V_v^{1/2} = 0.695 V_v^{1/2}, \quad (39)$$

where the  $\mu_i$ 's are the  $i$ th moments of the TLS distribution defined as

$$\mu_i = \frac{\int_0^\infty R^i F(R, t) dR}{\langle R \rangle' N_v}. \quad (40)$$

The coefficient on the r.h.s. of eq.(39) is slightly different from that appearing in eq.(25), because these coefficients reflect different combinations of the moments of the distribution function.

For the lower ranges of volume fraction the exponent appearing in Fig. 3 is 1/3, consistent with earlier simulations [13] and theories employing a cut-off radius based on the interparticle separation [16]. The rollover point between the two exponents depends on the number of particles,  $n$ , in the cluster, so that for clusters with larger  $n$  the transition occurs at progressively lower volume fractions. To explain the observed rollover behavior we substitute eq. (2) into eq. (21). This yields the Debye screening length  $\Lambda_D$  in terms of volume fraction  $V_v$  as

$$\Lambda_D = 3^{-1/2} \left( \langle R^3 \rangle / \langle R \rangle \right)^{1/2} (V_v)^{-1/2}. \quad (41)$$

The spatial extent of the cluster,  $\Lambda_{\text{tot}}$ , can also be estimated in terms of  $V_v$  as

$$\Lambda_{\text{tot}} = (4\pi/3)^{-1/3} (n/N_v)^{1/3} = n^{1/3} \langle R^3 \rangle^{1/3} (V_v)^{-1/3}. \quad (42)$$

Comparison of eqs. (41) and (42) shows that the Debye screening distance grows faster with decreasing volume fraction than does the cluster size, holding other system parameters constant. This implies that at some small volume fraction,  $V_v^*$ , the Debye screening distance,  $\Lambda_D$ , exceeds the cluster size, and then diffusional screening is precluded.

When screening is no longer possible because of the sparsity of the cluster, then the deviations from TLS theory no longer have to be proportional to  $V_v^{1/2}$ . Indeed, comparing the TLS result, eq. (8), with the monopole expression, eq. (35), one obtains for the deviation from TLS:

$$\delta B_i = \left[ -\frac{R_i}{\lambda} \left( \sum_{j=1, j \neq i}^n \frac{B_j + \delta B_j}{|\mathbf{r}_j - \mathbf{r}_i|} \right) \right]. \quad (43)$$



For a sparse system,  $\delta B_i$  on the r.h.s. of eq. (43) may be neglected. The r.h.s. of eq. (43) may be then estimated, using the fundamental metric scales of the system, as  $B_i \Lambda_R / \Lambda_N$ . In terms of the volume fraction, one may express eq. (35) as

$$\frac{\delta B_i}{B_i} \approx -\frac{\Lambda_R}{\Lambda_N} \approx \frac{\langle R \rangle}{N^{-1/3}} = \frac{\langle R \rangle}{\langle R^3 \rangle^{1/3}} V_V^{1/3}. \quad (44)$$

Equation (44) shows that for extremely sparse clusters, the leading order deviation from TLS kinetics goes as  $V_V^{1/3}$ . This result is consistent with the asymptotic analysis performed in [12] for a periodic system.

The rollover point at which the exponent changes from 1/2 to 1/3 occurs when the Debye screening distance becomes comparable to the cluster size. The corresponding volume fraction,  $V_V^*$ , may be estimated from the condition  $\Lambda_{\text{tot}} = \Lambda_D$ , which with the use of eqs. (41) and (42) gives the result

$$V_V^* = \frac{\langle R^3 \rangle}{\langle R \rangle^3} \frac{1}{27n^2} \approx \frac{1}{27n^2}. \quad (45)$$

Figure 3 also shows the theoretical rollover points calculated from eq.(45) denoted by vertical arrows for clusters containing  $n=10$ , 100, and 1000 particles. The predictions from eq.(45) appear satisfactory for  $n=100$  and 1000, despite the fact that the clusters investigated here have relatively few particles to provide the Debye screening behavior. We note, that a cluster with 1000 particles contains only about 6 interparticle distances from its center to its periphery. The cluster containing 10 particles fails to show screening behavior for volume fractions approaching 1%. Diffusional interactions in clusters with volume fractions above about 1% would not be represented accurately by the monopole approximation.

## VI. Conclusions

1) Monopole snapshot calculations provide an efficient method for estimating the coarse-grained rate constants in finite clusters of coarsening particles. Prior to development of this technique, fully time-dependent simulations were required to obtain this information.

2) Extending the definition of volume fraction to a finite cluster permits investigating the influence of non-zero volume fraction on the coarsening kinetics.

3) The present results confirm that in finite clusters in the limit of low volume fraction the leading correction to the TLS rate constant is proportional to  $V_V^{1/3}$ . For higher volume fractions, or for a sufficient number of particles, Debye screening occurs and the leading-order term becomes proportional to  $V_V^{1/2}$ .

4) The rollover point between the two kinetic behaviors, that is, the critical volume fraction at which the Debye screening distance is comparable to the cluster size is given by eq.(45) and depends on the number of particles in the cluster. For clusters with only one

thousand particles, the rollover point is already as low as  $ca. 3 \cdot 10^{-8}$ . This implies that in most experimental coarsening systems  $V_v^{1/3}$  behavior should not occur.

5) Inasmuch as Debye screening is not directly applicable to small clusters, its apparent success in explaining the results of these calculations require further analysis. Larger-scale calculations with clusters containing much greater numbers of particles will be required to resolve this interesting issue, as well as to provide additional information on correlation effects and the influence of the cluster periphery on coarsening kinetics.

6) At volume fractions above  $ca. 1\%$ , particle interactions become more complex than can be described with monopole approximations and Debye screening. Other techniques that incorporate spatial correlations among the particles, shape changes, direct screening, and higher-order multipole interactions must be employed.

## Acknowledgements

The authors gratefully acknowledge the support provided by the National Science Foundation, Division of Materials Research, Washington, DC, under grant # DMR93-07725, and the NASA Marshall Space Flight Center, Huntsville, AL, under Cooperative Agreement NCC8-54. The authors also acknowledge the contributions of Dr. V. Belsky concerning numerical algorithms, and Mr. M. Rutman, who assisted in carrying out the programming and the numerical calculations.

## References

1. O. M. Todes, J. Phys. Chem (Sov.) **20**, 629 (1946).
2. I. M. Lifshitz and V. V. Slyozov, J. Phys. Chem. Solids **19**, 35 (1961).
3. P. W. Voorhees, J. Stat. Phys. **38**, 231 (1985).
4. P. W. Voorhees, Ann. Rev. Mat. Sci. **22**, 197 (1992).
5. Y. Enomoto, M. Tokuyama, and K. Kawasaki, Acta Met. **35**, 907 (1987).
6. J. A. Marqusee and J. Ross, J. Chem. Phys. **80**, 536 (1984).
7. J. A. Marqusee, J. Chem. Phys. **81**, 976-981 (1984).
8. B. K. Chakraverty, J. Phys. Chem. Solids **28**, 2401-2412 (1967).
9. S. P. Marsh, M. E. Glicksman, and D. B. Dadyburjor, J. Catalysis **99**, 358-374 (1986).
10. Y. Enomoto, M. Tokuyama, and K. Kawasaki, Acta Met. **34**, 2119 (1986).
11. J. J. Weins and J. W. Cahn, (Plenum, New York, 1973), p. 151.
12. P. W. Voorhees and M. E. Glicksman, Acta Met. **32**, 2001-2011 (1984).
13. P. W. Voorhees and M. E. Glicksman, Acta Met. **32**, 2013-2030 (1984).
14. J. R. Rogers, J. P. Downey, W. K. Witherow, *et al.*, J. of Electronic Materials **23**, 841-848 (1994).

15. V. E. Fradkov, S. S. Mani, M. E. Glicksman, *et al.*, J. of Electronic Materials **23**, 849-855 (1994).
16. S. P. Marsh, Ph. D. Thesis, Rensselaer Polytechnic Institute, Troy, NY, 1989.
17. K. Tsumuraya and Y. Miyata, Acta Met. **31**, 437-452 (1983).

## Figure Captions

1. Behavior of the denominator,  $\mathcal{D}$ , of eq.(15):
  - (a)  $\alpha > (2/3)^{2/3}$ ;
  - (b)  $\alpha = (2/3)^{2/3}$ ;
  - (c)  $\alpha < (2/3)^{2/3}$ .
2. Instantaneous and coarse-grained time dependence of the average particle size observed in computer simulation of mixed-dimensional cluster coarsening [14, 15].
3. Relative deviation,  $\Delta$ , of the kinetic rate constant for coarsening of finite clusters at various volume fractions from that at zero volume fraction. These data are obtained by snap-shot monopole calculations. Theory refers to eq.(39). Arrows correspond to the roll-over volume fractions where the exponent changes from  $1/3$  to  $1/2$ , as predicted by eq.(45).

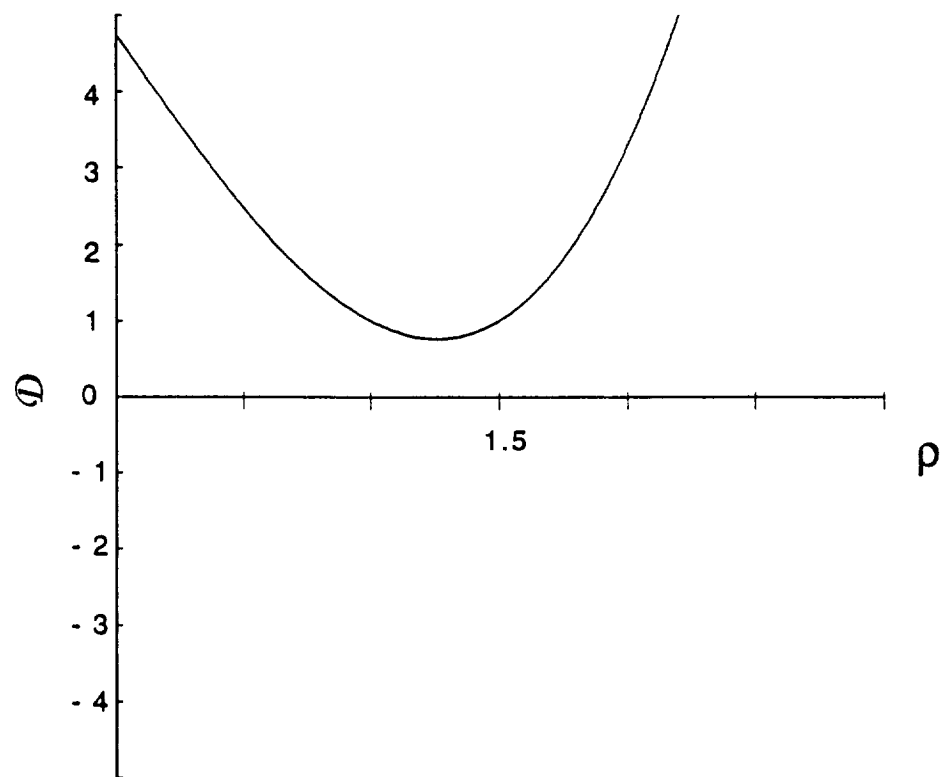


*figure 1a*

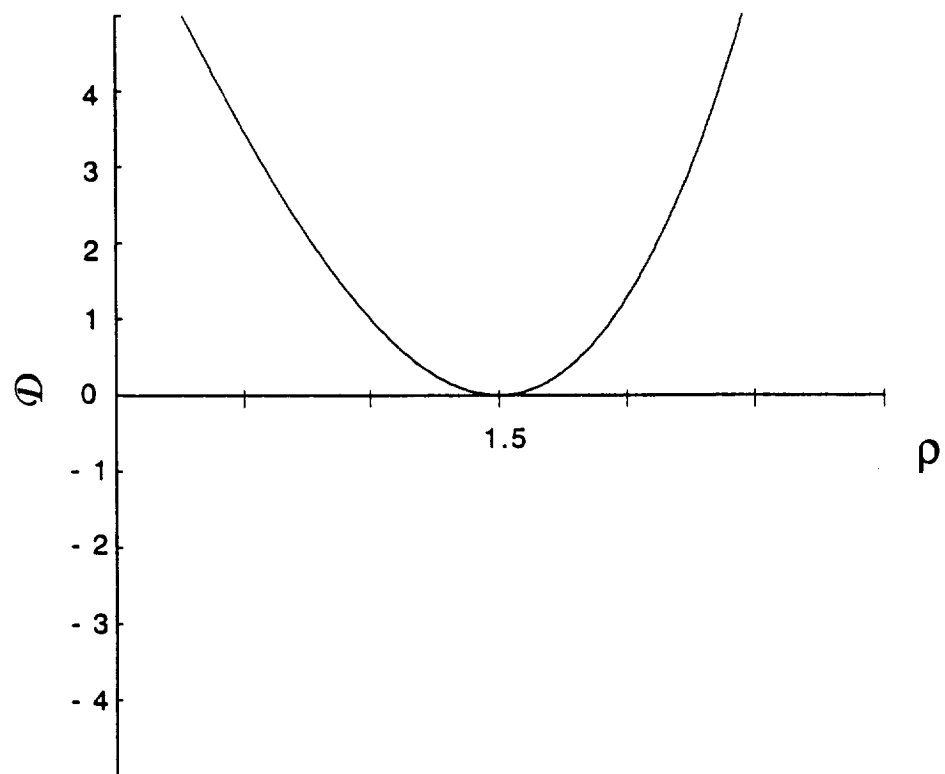


*figure 1b*

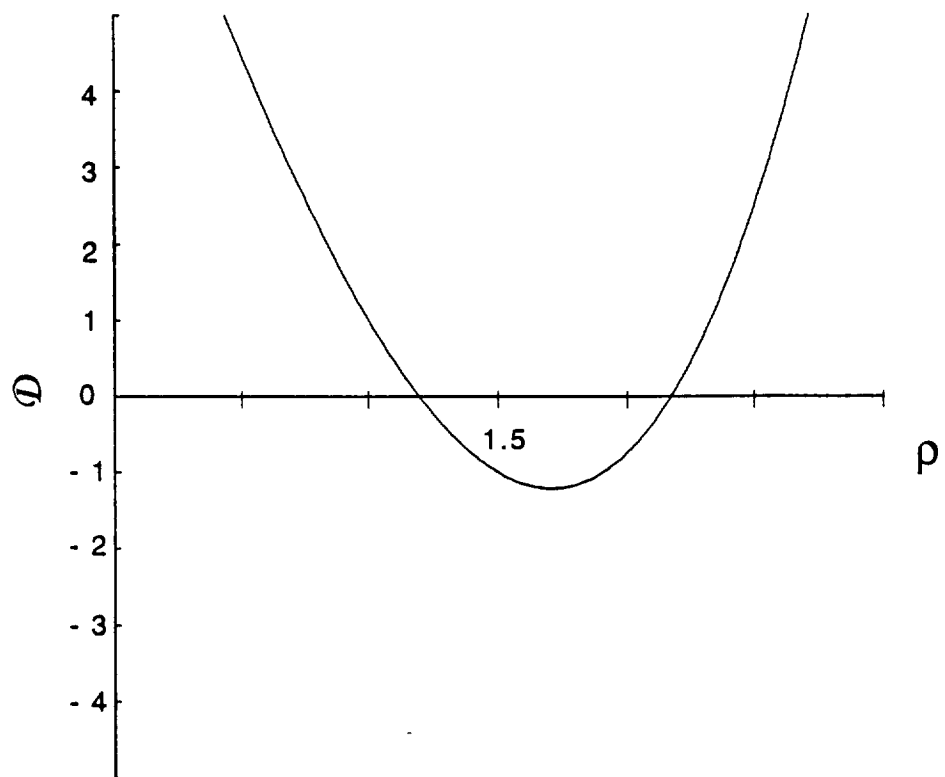


*figure 1c*

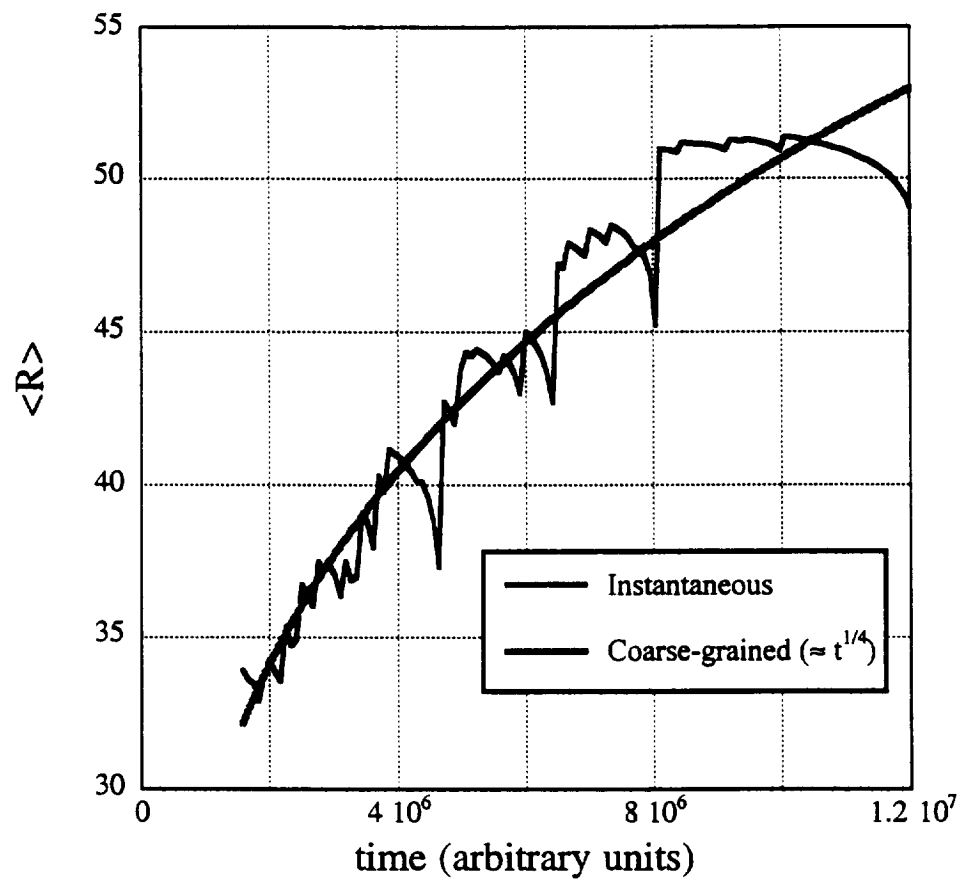


*figure 2*

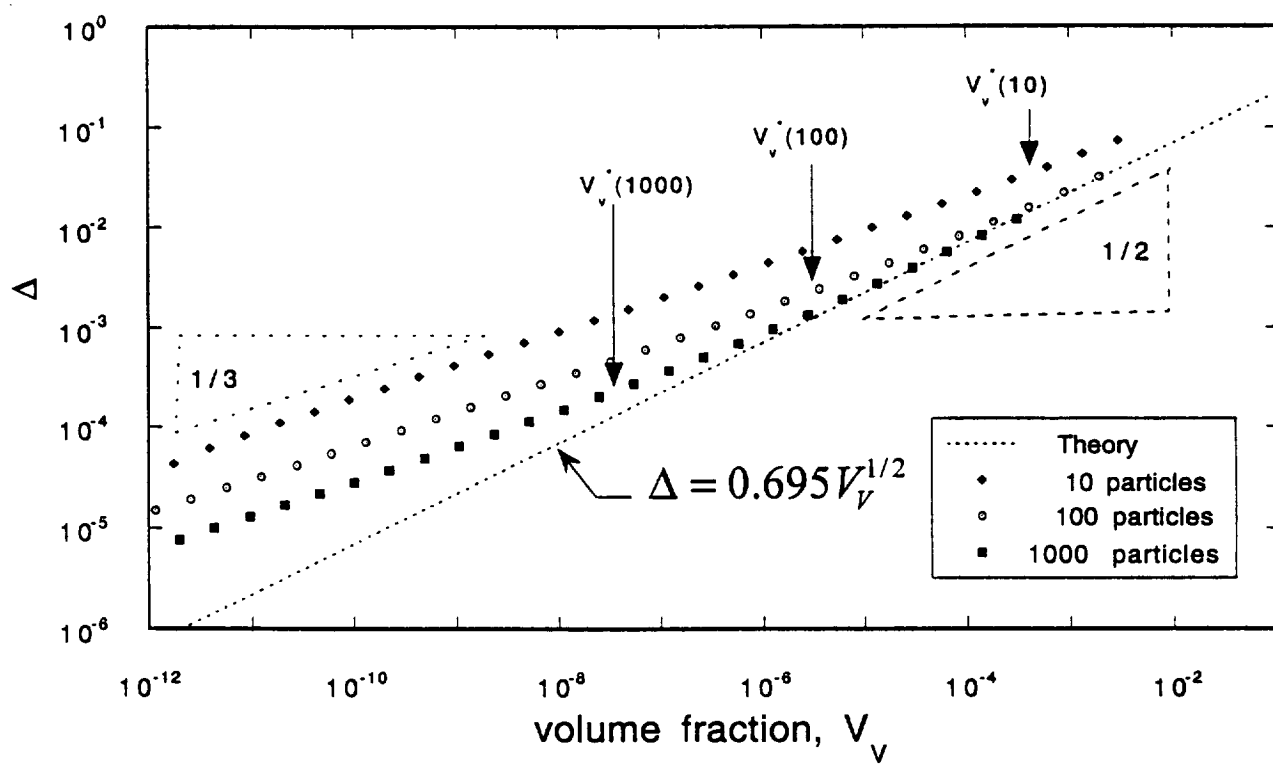


figure 3